Organic holographic polymer dispersed liquid crystal distributed feedback laser from different diffraction orders

2016 J. Phys. D: Appl. Phys. 49 465102

(http://iopscience.iop.org/0022-3727/49/46/465102)

IOP Publishing Journal of Physics D: Applied Physics
J. Phys. D: Appl. Phys. **49** (2016) 465102 (8pp) doi:10.1088/0022-3727/49/46/465102

Organic holographic polymer dispersed liquid crystal distributed feedback laser from different diffraction orders

Minghuan Liu[1,2], Yonggang Liu[1], Guiyang Zhang[1,2], Zenghui Peng[1], Dayu Li[1], Ji Ma[1,3] and Li Xuan[1,4]

[1] State Key Laboratory of Applied Optics, Changchun Institute of Optics, Fine Mechanics and Physics, Chinese Academy of Sciences, Changchun 130033, People's Republic China
[2] University of Chinese Academy of Sciences, Beijing 100049, People's Republic China
[3] Liquid Crystal Institute, Kent State University, Kent, OH 44240, USA

E-mail: liuminghuan13@mails.ucas.ac.cn, liuyg@ciomp.ac.cn, 478368204@qq.com, peng@ciomp.ac.cn, lidayu@ciomp.ac.cn, jma2@kent.edu and xuanli@ciomp.ac.cn

Received 19 July 2016, revised 26 September 2016
Accepted for publication 30 September 2016
Published 24 October 2016

Abstract

Holographic polymer dispersed liquid crystal (HPDLC) based distributed feedback (DFB) lasers were prepared with poly (-methoxy-5-(2′-ethyl-hexyloxy)-1,4-phenylene-vinylene) (MEH-PPV) film as the active medium layer. The HPDLC grating film was fabricated via holographic induced photopolymerization. The pure film spectra of MEH-PPV and the amplified spontaneous emission (ASE) spectrum were investigated. The laser device was single-longitudinal mode operation. The tunability of the HPDLC DFB laser was achieved by selecting different grating periods. The lasing performances were also characterized and compared from different diffraction orders. The lasing threshold increased with the diffraction order and the third order laser possessed the largest conversion efficiency in this device. The experimental results were in good agreement with the theoretical calculations.

Keywords: distributed feedback lasers, holographic polymer dispersed liquid crystal, diffraction order

(Some figures may appear in colour only in the online journal)

1. Introduction

Organic distributed feedback (DFB) lasers based on holographic polymer dispersed liquid crystal (HPDLC) have attracted more and more attention recently [1–5]. DFB HPDLC lasers use organic laser dyes or/and conjugated polymers [6–10] as active medium materials and HPDLC grating film is used as the DFB oscillation cavity, which make them compact, tunable, versatile and cost-effective for wide spectrum covering devices [11–13].

DFB configurations [14–16] are extensively used as the laser oscillation cavity because they render extremely low threshold operation and superior spectrum compression [10, 11]. The conjugated polymer film based DFB HPDLC laser combines the predominant properties of HPDLC grating film and organic semiconductors, which make them outstanding smart laser sources. So far, there are insufficient investigations on the laser emission from different diffraction orders for DFB HPDLC lasers. Such work can make insights into the lasing mechanism and obtain comprehensive understanding for HPDLC DFB lasers.

In this study, the conjugated polymer poly(-methoxy-5-(2′-ethyl-hexyloxy)-1,4-phenylene-vinylene) (MEH-PPV) film based DFB HPDLC laser was fabricated. The pure film spectra of MEH-PPV such as absorbance and photoluminescence (PL) were studied. The ASE spectrum was collected and the tunability of the HPDLC DFB laser was characterized. The laser emission and the far-field emission pattern of the emitting beams from different diffraction orders were investigated and compared. The lasing mechanism was analyzed and discussed.

[4] Author to whom any correspondence should be addressed.

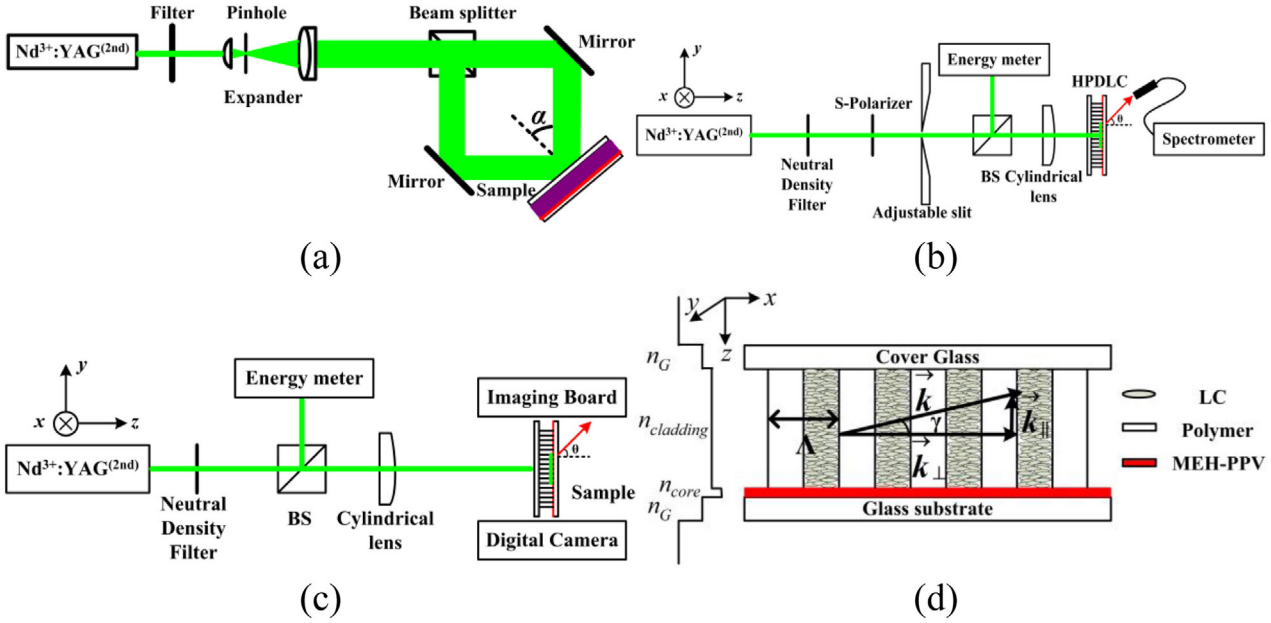

Figure 1. Experimental setup of (a) HPDLC grating film fabrication, (b) lasing performance characterization of the HPDLC DFB laser and (c) the far-field emission pattern of the emitting beam collection from the HPDLC DFB laser. (d) Schematic of HPDLC DFB laser device configuration.

2. Experiment

2.1. Sample preparation

The holographic mixture [17, 18], which contained acrylate monomers (dipentaerythritol hydroxyl pentaacrylate (DPHPA, Aldrich, 29.4wt.%) and phthalicdiglycoldiacrylate (PDDA, Eastern Acrylic Chem, 29.4wt.%)), nematic liquid crystals (TEB-30A, $n_o = 1.522$, $\Delta n = 0.170$, Silichem, 29.4 wt.%), crosslinking monomer N-vinylpyrrolidone (NVP, Aldrich, 9.8wt.%), photoinitiator Rose Bengal (RB, Aldrich, 0.5wt.%) and coinitiator N-phenylglycine (NPG, Aldrich, 1.5wt.%), was prepared to fabricate HPDLC grating film. The holographic mixture was stirred for 36 h in a darkroom to ensure a homogeneous material system.

The MEH-PPV film was used as the active medium layer [19, 20]. The MEH-PPV (Polymer Light Technology) was dissolved in tetrahydrofuran (THF) by weight ratio at 0.6wt.%, after which the MEH-PPV/THF solution was stirred for 72 h to ensure sufficient dissolution. A drop of MEH-PPV solution was injected on a piece of deionized pre-clean glass substrate for spin-coating MEH-PPV film. The thickness of the MEH-PPV film was controlled by spin speed and confirmed by surface profiler (KLA Tencor P-16+).

The empty cell was fabricated with two pieces of glass plates, one had MEH-PPV film coating and the other was a pure glass plate. The cell gap was controlled by Mylar spaces at 9 μm. The holographic mixture was injected into an empty sample cell by capillary action in the darkroom. All the experiments were performed at room temperature.

2.2. Pure film spectra characterization of MEH-PPV

The pure film spectra of MEH-PPV were investigated to obtain the absorbance and photoluminescence properties of the gain medium MEH-PPV. The absorbance spectrum of the spin-coating MEH-PPV film was performed by UV-3101PC (SHIMADZU) spectrometer and the photoluminescence spectrum was performed by a F-7000FL (Hitachi) spectrometer. For absorbance, the sampling wavelength was from 380 to 700 nm, and the sampling interval was 0.2 nm. For PL, the xenon light was used as the excitation light source. The excitation wavelength was settled at 500 nm to match the maximum absorbance of MEH-PPV. The initial and the end sampling wavelengths were 510 and 750 nm, respectively, and the sampling interval was 0.2 nm. To eliminate the waveguide effect [21], the film thickness for pure film spectra characterization was controlled below 50 nm.

2.3. HPDLC grating film fabrication

The HPDLC grating film was fabricated by holography induced photo-polymerization [22–29], which was used as the DFB oscillation cavity. The sample was photo-cured by illuminating the sample cell for 60 s by two continuous frequency doubled neodymium-doped yttrium aluminum garnet (Nd^{3+}:YAG) laser beams (New Industries Optoelectronics), as shown in figure 1(a). A variable calibrated neutral density filter was inserted into the beam path to adjust the beam intensity. The recording intensity for recording the second, third, fourth, fifth and sixth order HPDLC film was 5.1, 3.15, 2.85,

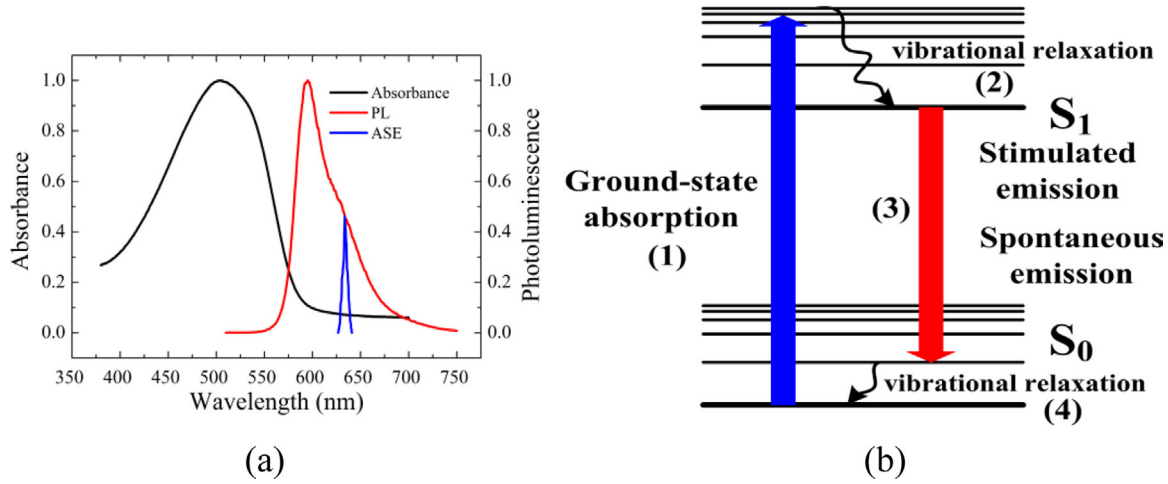

Figure 2. (a) Absorbance and photoluminescence spectra of the pure MEH-PPV film and ASE spectrum gathered from the DFB HPDLC device and (b) energy levels and transitions of the lowest two singlet states of an organic semiconductor material.

2.62 and 2.45 mW cm^{-2}, respectively. The beam expander, which contained a micro-objective (Newport, M-20X), a pinhole (Newport, PH-25) and a cemented doublet lens, was used to expand the recording beam and filter the recording beam spatially. After which, the sample was exposed by an ultraviolet (UV) light for 10 min to further stabilize the HPDLC grating film [30, 31]. The HPDLC film can also protect the MEH-PPV film from photo-induced oxidation and degradation [32–34] because the MEH-PPV film is sandwiched between the HPDLC grating film and glass substrate as shown in figure 1(d). The HPDLC film mainly contains alternate LC layers and polymer layers after photo-curing, as shown in figure 1(d). The spatial period of the HPDLC grating film is determined by

$$\Lambda = \frac{\lambda_{\mathrm{rec}}}{2\sin(\alpha)}, \qquad (1)$$

where Λ is the period of the HPDLC grating, λ_{rec} is the recording laser wavelength in vacuum, and α is the half intersection angle between two recording beams. Different grating periods can be obtained by varying the intersection angle in experiments. Figure 1(d) shows the device configuration. The gain medium MEH-PPV film was sandwiched between the HPDLC grating film and glass substrate. The pitch, i.e. the period of the HPDLC grating Λ is shown in figure 1(d). The MEH-PPV is used to amplify the light field while the HPDLC grating is used to provide feedback and spectrum selection for the laser device.

2.4. Lasing performance characterization

For the lasing performance characterization of the DFB HPDLC laser, the sample was transversely optical excited by a frequency-doubled Q-switched Nd^{3+}:YAG pulsed laser (532 nm, 10 ns, 10 Hz) (New Industries Optoelectronics), as shown in figure 1(b). The output lasing signal was collected with a fiber-coupled spectrometer (Sofn Instruments) with a resolution of ~0.3 nm. An s-polarizer was used to filter the exciting laser beam. The exciting laser beam was focused with a cylinder lens ($f = 200$ mm) to produce an 8 mm by 1 mm rectangle exciting area on the sample. An adjustable slit was used to select the central part (3 mm by 1 mm) of the pumping area to ensure uniform exciting. Moreover, a beam splitter (BS) was used in the beam path to split off one beam to monitor the exciting beam energy in real time. The variable neutral density filter was used to regulate the pump energy to investigate output-emission intensity as a function of excitation energy. For the far-field emission pattern of the emitting beams' acquisition from the DFB HPDLC laser, the emitting beams were imaged with an imaging board and recorded with a digital camera, as shown in figure 1(c).

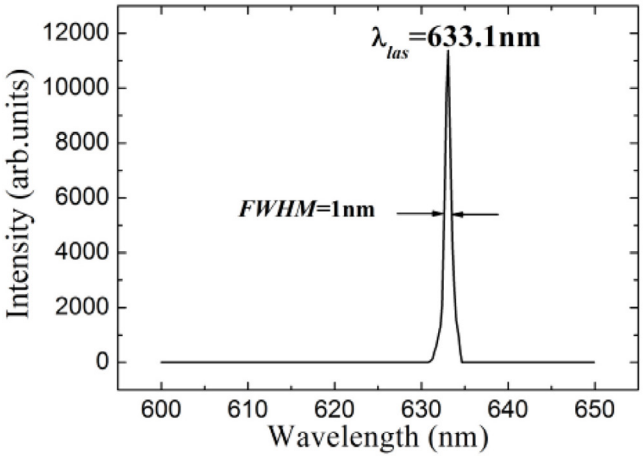

Figure 3. Typical lasing spectrum of DFB HPDLC laser collected from surface normal (396.9 nm period, second order).

3. Results and discussion

3.1. Pure film and amplified spontaneous emission (ASE) spectra characterization

Figure 2(a) shows the absorbance and PL spectra of pure MEH-PPV film. The peak of the absorbance spectrum located at 499 nm, where the absorbance was the maximum.

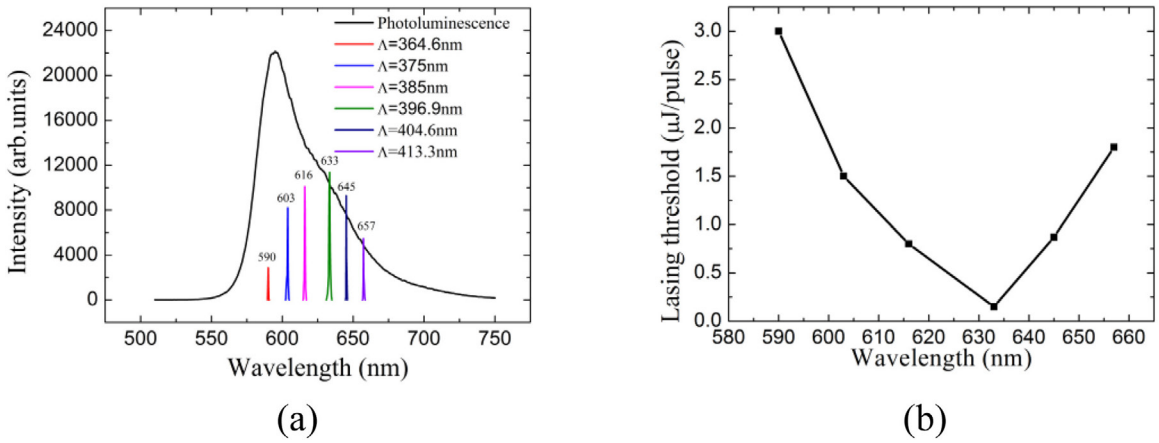

Figure 4. (a) Tunability of the HPDLC DFB laser by varying the grating period and (b) dependence of the lasing threshold to the lasing wavelength.

The absorbance at 532 nm was 90% of the maximum value. Therefore, the absorbance is sufficient when the sample is photo-pumped at 532 nm. The peaks of the PL spectrum represent vibronic structure, the 0–0 and 0–1 emission band. The S_{0-0} and S_{0-1} peak of the PL spectrum was centered at 594 and 634 nm, respectively. The narrow spectrum was the ASE spectrum, which was gathered from the DFB HPDLC laser sample edge. The central wavelength of the ASE was 633 nm, which is well matched for the S_{0-1} peak. During the photo-pumping, only the gain-narrowed (ASE) peak survived, and the broad tails of the photoluminescence were totally compressed when the gain exceeded the waveguide losses. Figure 2(b) represents the typical energy levels and transitions for the lowest two singlet states of an organic semiconductor material, such as MEH-PPV [10, 11]. The peak of the PL spectrum corresponds to the transition from S_{1-0} to S_{0-0}, which is detrimental for lasing operation. While the ASE spectrum corresponds to the transition from S_{1-0} to S_{0-1}, for the net gain is the largest among the gain spectrum. Therefore, selecting the lasing mode in the ASE spectrum is helpful for the buildup of lasing oscillation.

3.2. Lasing from the HPDLC DFB laser

In the DFB laser, feedback is provided by coherent Bragg scattering of the guided light via gain or/and index coupling [14–16]. The condition for feedback is given by the Laue condition [35]

$$2\vec{k}\cdot\vec{G} = \left|\vec{G}\right|^2, \tag{2}$$

where the wave-vector of the guided mode is $k = n_{\text{eff}}k_0$ (k_0 is the free-space vector number and n_{eff} is the effective index of the guided mode) and G denotes of the reciprocal lattice of the periodic dielectric structure with $G = m\cdot 2\pi\Lambda^{-1}$ (where m is an integer and Λ is the period). Substituting k and G to equation (2), it can be expressed as

$$2\cdot\left(n_{\text{eff}}\frac{2\pi}{\lambda_{\text{las}}}\right)\cdot\left(m\frac{2\pi}{\Lambda}\right) = \left(m\frac{2\pi}{\Lambda}\right)\cdot\left(m\frac{2\pi}{\Lambda}\right). \tag{3}$$

After simplification, equation (2) can be finally expressed as

Table 1. The emission angle with different diffraction orders.

Diffraction order	Grating period (nm)	n value	Emission angle (°)
2	396.9	1; −1	0,180
3	596.0	2; −1	32,148; −32, −148
4	793.7	3; −1	53,127; −53, −127
5	992.2	4; −1	73,107; −73, −107
6	1191.5	4; −2	32,148; −32, −148

$$m\lambda_{\text{las}} = 2n_{\text{eff}}\Lambda, \tag{4}$$

where λ_{las} is the lasing wavelength in vacuum. Different order HPDLC DFB lasers can be obtained by changing the grating period Λ in experiment. For $m > 1$, the lasing radiation is coupled out of the waveguide by an angle θ relative to the sample surface normal via grating coupling [36, 37]. Figure 3 shows the typical lasing spectrum of the DFB HPDLC laser with 396.9 nm period for second order, which was collected from the DFB HPDLC laser surface normal and the collection angle for third, fourth, fifth and sixth order laser was 32, 53, 73 and 32°, respectively. The central lasing wavelength was 633.1 nm and the full width at half maximum (FWHM) of the lasing spectrum was 1 nm. It is clear the laser device is single-longitudinal mode operation.

3.3. Tunability of DFB laser with HPDLC grating period

According to equation (4), for a given order m, the grating period can be selected to obtain varied lasing emission. Therefore, the gain spectra can be achieved. Here we chose $m = 2$ order. Figure 4(a) displays the tunability of DFB HPDLC laser by varying the grating period. The lasing signal was detected at 590, 603, 616, 633, 645 and 657 nm, which demonstrated a tunable range of 67 nm. The grating period was 367.6, 376.6, 385.5, 396.9, 404.6 and 413.3 nm in order to obtain the lasing signal of different wavelength.

Figure 4(b) is the dependence of lasing threshold on lasing wavelength. The lasing threshold for 590, 603, 616, 633, 645 and 657 nm laser was 3, 1.5, 0.8, 0.15, 0.9 and 1.8 μJ/pulse,

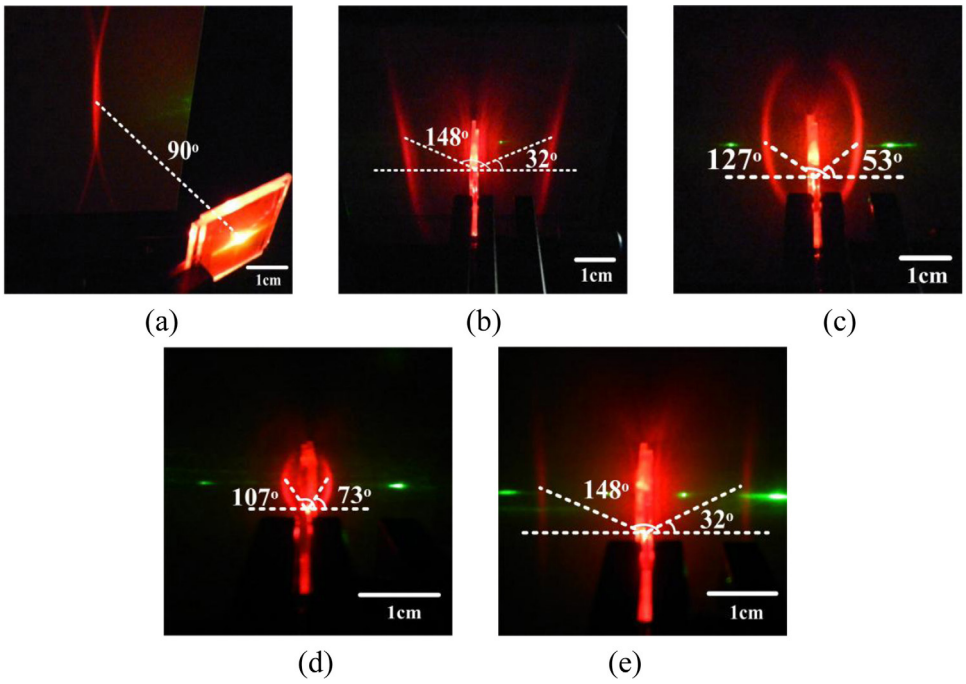

Figure 5. Far-field emission pattern of the emission beams from the DFB HPDLC laser for different diffraction orders, (a) $m = 2$, period = 396.9 nm (b) $m = 3$, period = 596.0 nm (c) $m = 4$, period = 793.7 nm (d) $m = 5$, period = 992.2 nm and (e) $m = 6$, period = 1191.5 nm. Images (a) and (b) were collected at an excitation of 10 μJ/pulse, images (c) and (d) were collected at an excitation of 20 μJ/pulse and image (e) was collected at an excitation of 30 μJ/pulse.

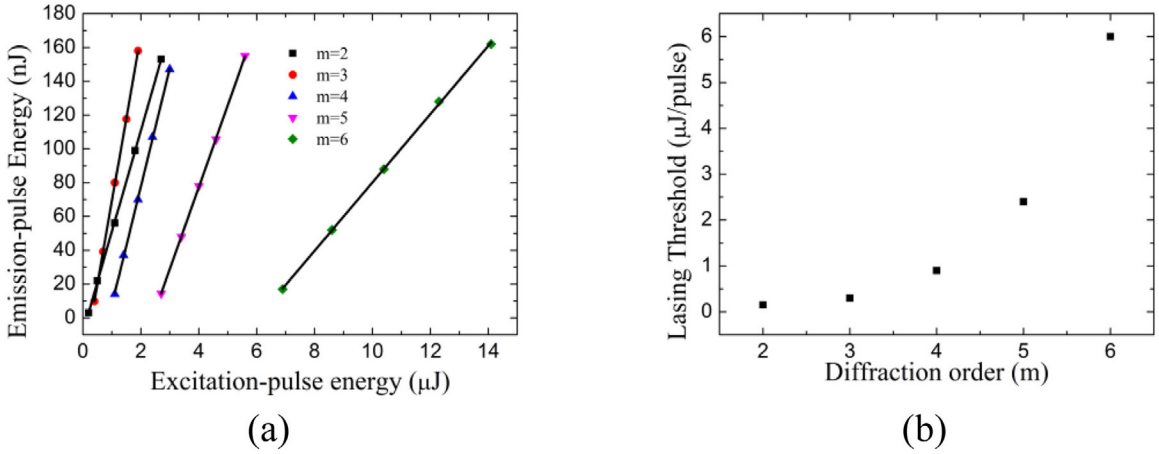

Figure 6. (a) Emission-pulse intensity with excitation-pulse energy and (b) lasing threshold from different diffraction orders.

respectively. The 633 nm lasing possesses the minimum lasing threshold. The lasing intensity can be described by

$$I(z) = I_0 \exp[(g_0(\lambda) - \alpha(\lambda))z], \tag{5}$$

where z is the distance when light travels across the active medium, I_0 is the initial intensity, $I(z)$ is the intensity when light travels in the active medium at a distance of z, $g_0(\lambda)$ and $\alpha(\lambda)$ is the small-signal gain and losses parameters, respectively. The losses parameter $\alpha(\lambda)$ mainly contains scatterings and self-absorbance. The small-signal gain parameter $g_0(\lambda)$ is wavelength dependent, which becomes maximum when the lasing spectrum is in the ASE spectrum. It is understandable that the 633 nm lasing possess the minimum threshold for the net gain that is the largest. For shorter wavelengths of less than 633 nm, the small-signal gain parameter $g_0(\lambda)$ becomes smaller and the self-absorbance becomes much more intense, so the lasing threshold increases. While for longer wavelength ranges of more than 633 nm, the small-signal gain parameter $g_0(\lambda)$ becomes smaller, so the lasing threshold also increases. In addition, the absorbance of MEH-PPV is so strong that there was not enough net gain to support the oscillation of the lasing mode for laser wavelengths lower than 590 nm. While for lasing wavelengths over than 657 nm, the photoluminescence of MEH-PPV is not sufficient to support the buildup of any lasing mode. The tunable range could be increased by using guest–host doping materials [38].

3.4. Tunability of the DFB laser with diffraction order

The light guided mode travelling in the waveguide [37] can be expressed as

$$k^2 = (nG_0 - k_0 \sin\theta)^2, \quad (6)$$

where n is an integer and varies with the diffraction order m, G_0 is equal to $*2\pi\Lambda^{-1}$. Equation (6) can be expressed as $\sin\theta = n\lambda_{las}/\Lambda - n_{eff}$ and $\sin\theta = n\lambda_{las}/\Lambda + n_{eff}$. There is a definition that $\theta > 0°$when n is a positive integer, while $\theta < 0°$ when n is a negative integer. The lasing emission from different diffraction order m can be obtained by choosing the grating period according to equation (4). In order to ensure the lasing wavelength in the range of ASE of MEH-PPV, we selected the output lasing wavelength at 633 nm. The theoretical calculations of the emission angle relative to the sample normal for different order lasers are listed in table 1, where the value of n_{eff} and λ_{las} is 1.595 and 633 nm, respectively. For $m = 2$, there are two output beams while for $m > 2$, there are four output beams.

In HPDLC DFB laser, the feedback is not only provided for guided waves propagating perpendicular to the HPDLC grating grooves but also for waves propagating at an angle γ with respect to the grating vector, owing to the HPDLC grating is only 1D and there is insufficient of lateral confinement as shown in figure 1(d) [35]. In the absence of any lateral confinement, a broad spectrum of lateral modes with continuously varying $\vec{k}_{\parallel}$ for a fixed $\vec{k}_{\perp}$ is supported. Therefore, the laser emission occurs at a divergent angle, which is parallel to the grating grooves. The divergent beams can be illustrated by the far-field emission pattern in figure 5 for different orders.

Figure 5 shows the far-field emission patterns of the emission beams from a different order of the HPDLC DFB laser. For second order, the emission beams were along the surface normal of the HPDLC DFB laser. For the third to sixth order, the emission beams emitted at 32/148, 53/127, 73/107 and 32/148 degree relative to the surface normal direction. The emission beams behaved as a fan-like shape divergent stripe for all the orders and the transverse modes can be clearly distinguished. In addition, the emission angles and number of emission beams were in good agreement with the theoretical calculations made by equation (6) as shown in figure 5. The oscillations at different DFB orders should occur for other DFB configurations fabricated by imprinting [39–42], molding [43–47] and holographic ablation [48] process. However, most of the process is complicated, expensive and time-consuming while the HPDLC gratings possess advantages such as ease of fabrication, cost-effectiveness, mass production and high pattern fidelity, which is superior to the imprinting, molding and holographic ablation process [26].

Figure 6(a) shows the emission-pulse energy with excitation-pulse energy with different diffraction orders at lasing wavelength 633 nm. The conversion efficiency was 6.0%, 9.8%, 7.0%, 4.8% and 2.0% for the second, third, fourth, fifth and sixth order HPDLC DFB laser, respectively. Figure 6(b) is the lasing threshold from different diffraction orders. The lasing threshold increased with the diffraction order increasing. The lasing threshold was 0.15, 0.3, 0.9, 2.4 and 6 μJ/pulse for the second, third, fourth, fifth and sixth order HPDLC DFB laser, respectively. The experimental results indicate that the lasing threshold decreases when the HPDLC DFB laser operates at lower order while the third order HPDLC DFB laser possesses the maximum conversion efficiency. For non-surface lasing emission, i.e. lasers from third order or higher, we can see the conversion efficiency was 6.0%, 9.8%, 7.0%, 4.8% and 2.0% for third, fourth, fifth and sixth order, respectively. The lower the order, the higher the conversion efficiency [3].

4. Conclusions

In conclusion, investigation was performed for the HPDLC DFB laser. The spin-coated MEH-PPV film was used as the active medium layer and the HPDLC grating film was fabricated on the MEH-PPV film as the DFB oscillation cavity. The tunability of the HPDLC DFB laser was achieved by changing grating periods, which had a tunable range of 67 nm. The lasing performances were also investigated and compared from different diffraction orders. The lasing threshold increased with diffraction orders while the third order laser possessed the maximum conversion efficiency in our device. The far-field emission pattern and the emission angle were in good agreement with theoretical calculations. This work gives more understanding on DFB HPDLC laser performance.

Acknowledgment

This work is supported by the National Natural Science Foundation of China (61377032 and 61378075). We thank Xinghai Lu and Zhongxu Cui of State Key Laboratory of Applied Optics for the testing.

References

[1] Criante L, Lucchetta D E, Vita F, Castagna R and Simoni F 2009 Distributed feedback all-organic microlaser based on holographic polymer dispersed liquid crystals *Appl. Phys. Lett.* **94** 111114

[2] Lucchetta D E, Vita F, Castagna R, Francescangeli O and Simoni F 2012 Laser emission based on first order reflection by novel composite polymeric gratings *Photonics Nanostruct.* **10** 140–5

[3] Diao Z H, Deng S P, Huang W B, Xuan L, Hu L F, Liu Y G and Ma J 2012 Organic dual-wavelength distributed feedback laser empowered by dye-doped holography *J. Mater. Chem.* **22** 23331–4

[4] Huang W, Diao Z, Liu Y, Peng Z, Yang C, Ma J and Xuan L 2012 Distributed feedback polymer laser with an external feedback structure fabricated by holographic polymerization technique *Org. Electron.* **13** 2307–11

[5] Liu L J, Xuan L, Zhang G Y, Liu M H, Hu L F, Liu Y G and Ma J 2015 Enhancement of pump efficiency for an organic distributed feedback laser based on a holographic polymer dispersed liquid crystal as an external light feedback layer *J. Mater. Chem.* C **3** 5566–72

[6] Mhibik O, Forget S, Ott D, Venus G, Divliansky I, Glebov L and Chenais S 2016 An ultra-narrow linewidth solution-processed organic laser *Light Sci. Appl.* **5** e16026

[7] Guo C, Sun T, Cao F, Liu Q and Ren Z 2014 Metallic nanostructures for light trapping in energy-harvesting devices *Light Sci. Appl.* **3** e161

[8] Park B *et al* 2014 Surface plasmon excitation in semitransparent inverted polymer photovoltaic devices and their applications as label-free optical sensors *Light Sci. Appl.* **3** e222

[9] Lozano G, Rodriguez S R K, Verschuuren M A and Rivas J G 2016 Metallic nanostructures for efficient LED lighting *Light Sci. Appl.* **5** e16080

[10] Vannahme C, Dufva M and Kristensen A 2015 High frame rate multi-resonance imaging refractometry with distributed feedback dye laser sensor *Light Sci. Appl.* **4** e269

[11] Samuel I D W and Turnbull G A 2007 Organic semiconductor lasers *Chem. Rev.* **107** 1272–95

[12] Chenais S and Forget S 2012 Recent advances in solid-state organic lasers *Polym. Int.* **61** 390–406

[13] Grivas C and Pollnau M 2012 Organic solid-state integrated amplifiers and lasers *Laser Photonics Rev.* **6** 419–62

[14] Kogelnik H and Shank C 1971 Stimulated emission in a periodic structure *Appl. Phys. Lett.* **18** 152–4

[15] Shank C, Bjorkholm J and Kogelnik H 1971 Tunable distributed-feedback dye laser *Appl. Phys. Lett.* **18** 395–6

[16] Kogelnik H and Shank C V 1972 Coupled-wave theory of distributed feedback lasers *J. Appl. Phys.* **43** 2327–35

[17] Huang W, Diao Z, Yao L, Cao Z, Liu Y, Ma J and Xuan L 2013 Electrically tunable distributed feedback laser emission from scaffolding morphologic holographic polymer dispersed liquid crystal grating *Appl. Phys. Express* **6** 022702

[18] Huang W, Liu Y, Hu L, Mu Q, Peng Z, Yang C and Xuan L 2013 Second-order distributed feedback polymer laser based on holographic polymer dispersed liquid crystal grating *Org. Electron.* **14** 2299–305

[19] Diao Z H, Xuan L, Liu L J, Xia M L, Hu L F, Liu Y G and Ma J 2014 A dual-wavelength surface-emitting distributed feedback laser from a holographic grating with an organic semiconducting gain and a doped dye *J. Mater. Chem.* C **2** 6177–82

[20] Diao Z, Kong L, Xuan L and Ma J 2015 Electrical control of the distributed feedback organic semiconductor laser based on holographic polymer dispersed liquid crystal grating *Org. Electron.* **27** 101–6

[21] DiazGarcia M A, Hide F, Schwartz B J, Andersson M R, Pei Q B and Heeger A J 1997 Plastic lasers: semiconducting polymers as a new class of solid-state laser materials *Synth. Met.* **84** 455–62

[22] Sutherland R L, Natarajan L V, Tondiglia V P and Bunning T J 1993 BRAGG Gratings in an acrylate polymer consisting of periodic polymer-dispersed liquid-crystal planes *Chem. Mater.* **5** 1533–8

[23] Sutherland R L, Tondiglia V P, Natarajan L V, Bunning T J and Adams W W 1994 Electrically switchable volume gratings in polymer-dispersed liquid-crystals *Appl. Phys. Lett.* **64** 1074–6

[24] Bunning T J, Natarajan L V, Tondiglia V P, Sutherland R L, Vezie D L and Adams W W 1995 The morphology and performance of holographic transmission gratings recorded in polymer-dispersed liquid-crystals *Polymer* **36** 2699–708

[25] Ma J, Huang W, Xuan L and Yokoyama H 2014 *Optical Properties of Functional Polymers and Nano Engineering Applications* ed V Jain and A Kokil (Boca Raton, FL: CRC Press)

[26] Bunning T J, Natarajan L V, Tondiglia V P and Sutherland R L 2000 Holographic polymer-dispersed liquid crystals (H-PDLCs) *Annu. Rev. Mater. Sci.* **30** 83–115

[27] Liu Y J, Dai H T and Sun X W 2011 Holographic fabrication of azo-dye-functionalized photonic structures *J. Mater. Chem.* **21** 2982–6

[28] De Sio L, Ricciardi L, Serak S, La Deda M, Tabiryan N and Umeton C 2012 Photo-sensitive liquid crystals for optically controlled diffraction gratings *J. Mater. Chem.* **22** 6669–73

[29] Peng H Y, Chen G N, Ni M L, Yan Y, Zhuang J Q, Roy V A L, Li R K and Xie X L 2015 Classical photopolymerization kinetics, exceptional gelation, and improved diffraction efficiency and driving voltage in scaffolding morphological H-PDLCs afforded using a photoinitibitor *Polym. Chem.* **6** 8259–69

[30] Huang W, Deng S, Li W, Peng Z, Liu Y, Hu L and Xuan L 2011 A polarization-independent and low scattering transmission grating for a distributed feedback cavity based on holographic polymer dispersed liquid crystal *J. Opt.* **13** 085501

[31] Huang W, Liu Y, Diao Z, Yang C, Yao L, Ma J and Xuan L 2012 Theory and characteristics of holographic polymer dispersed liquid crystal transmission grating with scaffolding morphology *Appl. Opt.* **51** 4013–20

[32] Persano L, Camposeo A, Carro P D, Solaro P, Cingolani R, Boffi P and Pisignano D 2009 Rapid prototyping encapsulation for polymer light-emitting lasers *Appl. Phys. Lett.* **94** 123305

[33] Herrnsdorf J *et al* 2010 Flexible blue-emitting encapsulated organic semiconductor DFB laser *Opt. Express* **18** 25535–45

[34] Vannahme C, Klinkhammer S, Christiansen M B, Kolew A, Kristensen A, Lemmer U and Mappes T 2010 All-polymer organic semiconductor laser chips: parallel fabrication and encapsulation *Opt. Express* **18** 24881–7

[35] Riechel S, Lemmer U, Feldmann J, Benstem T, Kowalsky W, Scherf U, Gombert A and Wittwer V 2000 Laser modes in organic solid-state distributed feedback lasers *Appl. Phys.* B **71** 897–900

[36] Ziebarth J M and McGehee M D 2003 Measuring the refractive indices of conjugated polymer films with Bragg grating out couplers *Appl. Phys. Lett.* **83** 5092–4

[37] Turnbull G A, Andrew P, Barnes W L and Samuel I D W 2003 Photonic mode dispersion of a two-dimensional distributed feedback polymer laser *Phys. Rev.* B **67** 165107

[38] Schneider D *et al* 2004 Ultrawide tuning range in doped organic solid-state lasers *Appl. Phys. Lett.* **85** 1886–8

[39] Berggren M, Dodabalapur A, Slusher R E, Timko A and Nalamasu O 1998 Organic solid-state lasers with imprinted gratings on plastic substrates *Appl. Phys. Lett.* **72** 410–1

[40] Reboud V, Lovera P, Kehagias N, Zelsmann M, Schuster C, Reuther F, Gruetzner G and Redmond G 2007 Two-dimensional polymer photonic crystal band-edge lasers fabricated by nanoimprint lithography *Appl. Phys. Lett.* **91** 151101

[41] Namdas E B, Tong M, Ledochowitsch P, Mednick S R, Yuen J D, Moses D and Heeger A J 2009 Low thresholds in polymer lasers on conductive substrates by distributed feedback nanoimprinting: progress toward electrically pumped plastic lasers *Adv. Mater.* **21** 799–80

[42] Whitworth G L, Zhang S, Stevenson J R Y, Ebenhoch B, Samuel I D W and Turnbull G A 2015 Solvent immersion nanoimprint lithography of fluorescent conjugated polymers *Appl. Phys. Lett.* **107** 163301

[43] Rogers J A, Meier M, Dodabalapur A, Laskowski E J and Cappuzzo M A 1999 Distributed feedback ridge waveguide lasers fabricated by nanoscale printing and molding on nonplanar substrates *Appl. Phys. Lett.* **74** 3257–9

[44] Lawrence J R, Turnbull G A and Samuel I D W 2003 Polymer laser fabricated by a simple micromolding process *Appl. Phys. Lett.* **82** 4023–5
[45] Lu M, Cunningham B T, ParkS J and Eden J G 2008 Vertically emitting, dye-doped polymer laser in the green (lambda similar to 536 nm) with a second order distributed feedback grating fabricated by replica molding *Opt. Commun.* **281** 3159–62
[46] Ge C, Lu M, Jian X, Tan Y F and Cunningham B T 2010 Large-area organic distributed feedback laser fabricated by nanoreplica molding and horizontal dipping *Opt. Express* **18** 12980–91
[47] Hermann S, Shallcross R C and Meerholz K 2014 Simple fabrication of an organic laser by microcontact molding of a distributed feedback grating *Adv. Mater.* **26** 6019–23
[48] Stroisch M, Woggon T, Lemmer U, Bastian G, Violakis G and Pissadakis S 2007 Organic semiconductor distributed feedback laser fabricated by direct laser interference ablation *Opt. Express* **15** 3968–73